Demonstration of Large Bandwidth Hard X-Ray Free-Electron Laser Pulses at SwissFEL

Eduard Prat,[1,*] Philipp Dijkstal,[1,2] Eugenio Ferrari,[1] and Sven Reiche[1]
[1]Paul Scherrer Institut, CH-5232 Villigen PSI, Switzerland
[2]ETH Zürich, CH-8093 Zürich, Switzerland

(Received 11 September 2019; revised manuscript received 12 December 2019; accepted 14 January 2020; published 21 February 2020)

We have produced hard x-ray free-electron laser (FEL) radiation with unprecedented large bandwidth tunable up to 2%. The experiments have been carried out at SwissFEL, the x-ray FEL facility at the Paul Scherrer Institute in Switzerland. The bandwidth is enhanced by maximizing the energy chirp of the electron beam, which is accomplished by optimizing the compression setup. We demonstrate continuous tunability of the bandwidth with a simple method only requiring a quadrupole magnet. The generation of such broadband FEL pulses will improve the efficiency of many techniques such as x-ray crystallography and spectroscopy, opening the door to significant progress in photon science. It has already been demonstrated that the broadband pulses of SwissFEL are beneficial to enhance the performance of crystallography, and further SwissFEL users plan to exploit this large bandwidth radiation to improve the efficiency of their measurement techniques.

DOI: 10.1103/PhysRevLett.124.074801

The recent advent of x-ray free-electron lasers (FELs) has triggered a scientific revolution, allowing the investigation of matter with spatial and time resolutions at the atomic level [1–7]. X-ray FEL facilities are typically based on the SASE process [8,9] starting from the shot noise of the electron beam. The SASE-FEL radiation is not fully coherent in the longitudinal direction of the beam: the achievable relative bandwidth is of the order of the Pierce parameter [9], which is between 10^{-4} and 10^{-3} for x-rays. FEL facilities normally minimize the bandwidth of the generated radiation to achieve maximum brightness. In fact, several methods such as self-seeding are being pursued [10–12] with the aim to generate fully coherent FEL pulses with smaller bandwidth than the values naturally given by the SASE process.

While many experiments take advantage of the higher coherence and reduced bandwidth, certain applications would benefit from FEL radiation with larger bandwidth. For example, the efficiency of x-ray crystallography [13–15], x-ray emission and absorption spectroscopy [16], stimulated-Raman spectroscopy [14], and multi-wavelength anomalous diffraction [17] would significantly improve with broad-brand FEL radiation. Hence, the generation of large bandwidth FEL pulses would open the door to outstanding developments in research areas such as material science and biology. From an operation perspective, a large bandwidth would allow a higher flexibility in the use of the photon beam: the radiation wavelength could be adjusted using monochromators without the need to tune any parameter on the machine side. Furthermore, FEL multiplexing [18,19] could allow an increased number of experiments to be performed in parallel.

The central wavelength of the FEL radiation is given by the following equation [9]:

$$\lambda = \frac{\lambda_u}{2\gamma^2}\left(1+\frac{K^2}{2}\right), \tag{1}$$

where λ_u is the undulator period length, γ is the Lorentz factor of the electron beam, and K is the undulator field parameter. The most natural way to generate broadband FEL radiation is to drive the FEL process with an electron beam with a large energy chirp, i.e., a beam with a strong correlation between the energy and the longitudinal coordinates of the electrons. According to Eq. (1), different longitudinal parts or slices of an energy-chirped beam will generate radiation at different wavelengths depending on the slice energy. For example, if the beam has a relative energy chirp of 1%, the radiation will ideally have a relative bandwidth of 2%. Alternatively, broadband FEL pulses could be achieved with a transversely chirped electron beam traveling through an undulator with transverse gradient [20,21]. In the following, we will focus only on producing large bandwidth radiation with energy-chirped electron beams. Besides the fact that it is a more straightforward approach, generating beams with large energy chirp improves the tunability of the methods to generate two-color FEL pulses based on energy-chirped beams—see for instance Refs. [22–24].

In the standard operation of an x-ray FEL facility, the longitudinal wakefields of the radio frequency (rf) linac compensate the energy chirp used for compression, such that the final energy chirp at the undulator entrance is minimized. One possibility to generate a large energy chirp is to change the sign of the chirp in the last bunch

compressor in the so-called *overcompression* regime, in such a way that the linac wakefields add to the final chirp of the electron beam [25,26]. The chirp could be additionally enhanced by optimizing the longitudinal profile of the photoinjector laser [26,27]. Another way to increase the energy chirp is to exploit the wakefields of dedicated passive devices such as corrugated or dielectric structures [28–30]. The chirp could also be enlarged by operating the rf structures of the facility at off-crest acceleration. This last approach is, however, rather inefficient in terms of rf power, in particular when considering that the electron beams required to produce FEL radiation in the x-ray regime have relatively large energies (in the gigaelectronvolt range) and short durations (of a few tens of femtoseconds or less).

FEL radiation with 15% bandwidth was produced for wavelengths at the micrometer level using an energy-chirped beam with a central beam energy of 70 MeV [31]. For x-rays the beam energy needs to be two orders of magnitude larger, thus rendering the generation of large energy chirps more challenging. The Linac coherent light source (LCLS) recently produced FEL radiation with a FWHM (full width at half maximum) bandwidth of 1.3% for a radiation wavelength of 1.5 Å (with an electron beam energy of 14 GeV) [32], and bandwidths up to 2% have been obtained for soft x-rays [33] at a beam energy of around 6 GeV (larger bandwidths are easier to achieve for soft x-rays, since for longer wavelengths the beam energy is normally reduced and therefore the relative energy chirp increases by default). Here we present the generation of large bandwidth x-ray pulses at SwissFEL [7] using an electron beam with a large energy chirp. We follow the procedure presented and simulated in Ref. [26]: the energy chirp is maximized by optimizing the compression setup and utilizing the wakefields of the linac.

In the large bandwidth mode the total pulse energy and pulse duration are in principle not affected in comparison to the standard operation mode (as shown later). Therefore, the FEL brightness remains the same. However, the spectral brightness or brilliance is reduced in proportion to the bandwidth increase. Tuning the bandwidth of the produced FEL radiation is a key operational aspect. One possibility is to adjust the compression parameters to increase or reduce the chirp up to some extent. This option is limited by the machine and electron parameters such as the minimum bunch compressor angles, the final required electron peak current, and the maximum electron beam charge. A more straightforward approach, demonstrated here, consists in inducing a transverse tilt to the electron beam [33]. In this case, the head and the tail of a transversely tilted beam will undergo betatron oscillations in the undulator and therefore will not lase—only the central part of the bunch with aligned trajectory will generate FEL radiation. Consequently, the spectral bandwidth will be reduced, but also pulse energy and duration will decrease accordingly. With this method the bandwidth can be adjusted continuously from the maximum achievable bandwidth to the minimum, defined by the Pierce parameter. This approach is very simple and can be achieved, for instance, by adjusting a quadrupole magnet in a dispersive section.

Figure 1 shows a sketch of the SwissFEL facility. Electron bunches with an energy of 7 MeV, typical charges of 200 pC and peak currents of 20 A are generated in an rf *S*-band (3 GHz) photoinjector. After that, an *S*-band booster accelerates the beam to an energy of about 300 MeV. The main linac consists of *C*-band (5.7 GHz) rf structures, which accelerate the electron beam to its final energy up to about 6 GeV. The beam is longitudinally compressed in two bunch compressors (BC1 and BC2). An *x*-band cavity (12 GHz) is used to linearize the compression. SwissFEL has two transverse-deflecting structures (TDS) to diagnose the longitudinal properties of the beam [34]. An energy collimator is placed before the undulator (more details will be given later). Further information about SwissFEL can be found in Ref. [7]. SwissFEL recently achieved its design parameters, producing FEL radiation for wavelengths down to 1 Å with a repetition rate up to 100 Hz [35].

The method to generate broadband pulses employed here could also be used at other facilities. Nevertheless, for the generation of large energy chirps, SwissFEL has two advantages over most other existing x-ray FEL facilities. First, it is driven by a relatively low energy beam compared to other facilities. Therefore the same absolute energy chirp corresponds to a higher relative chirp at SwissFEL. Second, the SwissFEL main linac operates at a frequency (5.7 GHz) higher than the standard *S*-band frequency. Consequently, the wakefield contributions to the final energy chirp are higher in our case.

Figure 2 shows examples of longitudinal phase-space measurements of the electron beam for standard and large bandwidth operation. The measurements are done by streaking the beam with the TDS at the linac end and

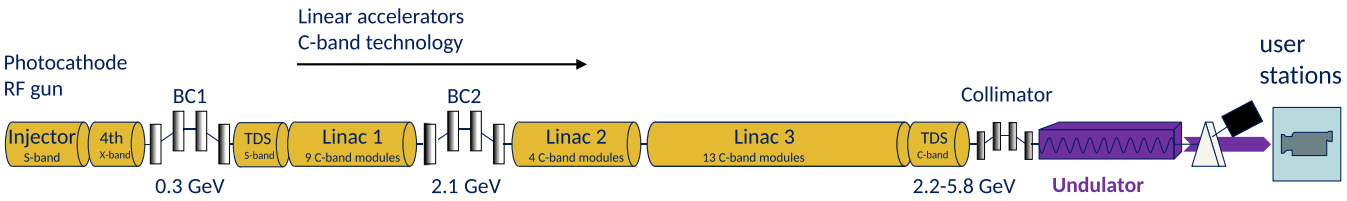

FIG. 1. SwissFEL schematic (not to scale).

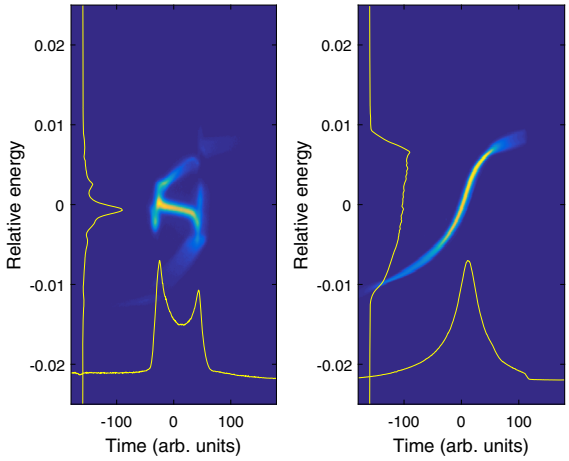

FIG. 2. Longitudinal phase-space measurement for standard (left) and large bandwidth (right) operation modes.

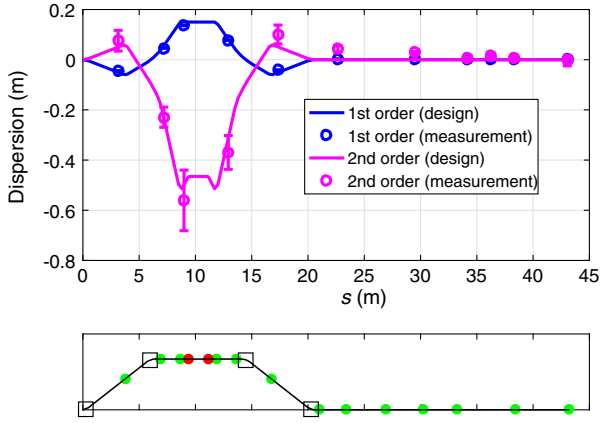

FIG. 3. Design and measured transverse dispersion at the beam-position monitors (circles) at the energy collimator. The bottom plot shows the lattice indicating dipole (black squares), quadrupole (green dots), and sextupole (red dots) magnets.

observing it with a scintillating screen at a dispersive section. The bunch charge is 200 pC, the mean beam energy is 5.5 GeV, and the measured rms pulse duration is between 25 and 30 fs for both cases. The FWHM energy chirp is 0.15% for the standard operation and 1.54% for the large bandwidth mode. In the standard setup for minimum bandwidth, the wakefields of the *C*-band linac compensate the energy chirp of the electron beam. For large bandwidth operation, however, the beam is overcompressed in BC2, i.e., the sign of the chirp is reversed in such a way that the wakefields add up to the final energy chirp.

The SwissFEL energy collimator is designed as a chicane, as opposed to the dog-leg configuration used by most other facilities. Its setup is crucial, as it must be isochronous in order not to change the compression. Specially for the large bandwidth mode, the longitudinal dispersion of a standard dispersive chicane would significantly decompress the electron beam, making it unsuitable for driving the FEL process. For this purpose, three pairs of quadrupoles are used to cancel both the longitudinal and transverse linear dispersions. Moreover, a pair of sextupole magnets is employed to compensate the second-order transverse dispersion generated at the quadrupole magnets. Figure 3 shows the design and measured first and second-order dispersion at the SwissFEL energy collimator and downstream. The dispersion is measured by recording the beam trajectory with beam-position monitors as a function of the electron beam energy, which is changed by varying the common accelerating phase of the linac-3 rf structures. The measured transverse dispersion in the energy collimator is well predicted by the model and fits the design values, ensuring that the collimator follows our isochronous design. Moreover, the dispersion after the collimator is closed to avoid any energy dependence of the lasing trajectory. To reach the nominal dispersion, the magnetic strengths of the quadrupoles and sextupoles need some slight empirical adjustments (typically below the percent level) to compensate for beam energy or magnetic calibration errors.

When working in the overcompression scheme, the beam undergoes full compression in BC2, so coherent synchrotron radiation (CSR) effects [36,37] may significantly deteriorate the transverse beam quality. In particular, strong transverse beam tilts may be generated during bunch compression. Such tilts need to be measured and corrected to ensure that most of the bunch contributes to the FEL process and to the final bandwidth—but, as explained before and shown later, such tilts can be useful to reduce the bandwidth of the produced radiation. Following the method described in [38], we use quadrupole and sextupole magnets in the bunch compressors to compensate for first- and second-order beam tilts. Figure 4 shows a measurement of the current profile, slice emittance and misalignment

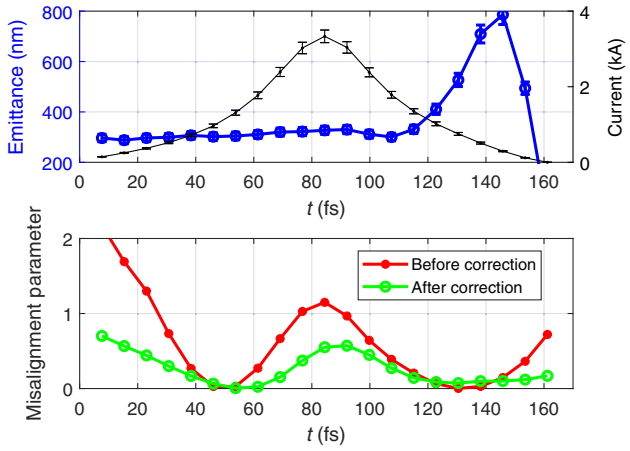

FIG. 4. Top: slice emittance (blue) and current profile (black) measurement of the electron beam. Bottom: slice misalignment parameter before (red) and after (green) applying beam tilt correction with quadrupole and sextupole magnets.

parameter of the electron beam when working in overcompression (we define the misalignment parameter as the invariant of motion associated to the measured slice trajectory offset and angle normalized by the slice emittance of the core [24]. According to simulations, lasing for a radiation wavelength of 1 Å and typical SwissFEL parameters is suppressed for a misalignment parameter above unity [24]). The conditions are the same as in the measurement shown in the right plot of Fig. 2. The emittance is determined at a scintillating screen using the quadrupole-scan technique [39]. The measured slice emittance for the core of the bunch (average over the five central slices) is about 300 nm, similar to the one measured for nominal standard compression, indicating that there is no significant degradation of the slice emittance from overcompression. The true slice emittance is in fact estimated to be about 100 nm less due to issues associated with profile monitor resolution [39]. At the tail of the bunch the slice emittance increases significantly. We attribute this increase to CSR effects in the bunch compressors. From Fig. 4 we see that the misalignment parameter is significantly reduced when applying beam tilt correction, staying well below unity for all longitudinal slices. After applying beam tilt correction, we observe that the pulse energy in the large bandwidth mode operation typically increases by 20–30%, indicating a significant bandwidth enhancement of the same order of magnitude.

The FEL spectra at SwissFEL are measured shot-to-shot using a spectrometer with a relative resolution between 2×10^{-5} and 5×10^{-5} and a field of view corresponding to about 0.5% of the radiation wavelength [40,41]. This is enough to measure spectra for standard operation but insufficient for the large bandwidth mode. To measure the broadband pulses we perform a monochromator scan and record the output intensity with a photodiode. The monochromator, located in the Bernina optical beamline of SwissFEL, consists of a double silicon crystal (Si-111) [42,43]. We verified that, for the standard operation case, the measurement using the shot-to-shot spectrometer agrees well with the monochromator scan.

Figure 5 displays the measured spectra of the FEL radiation produced with the electron beam shown in Figs. 2 and 4. The central radiation wavelength is around 1.55 Å. The uncertainty in the photon wavelength is estimated to be 0.015%. We show the spectrum for the standard and large bandwidth operation modes. For the latter, we demonstrate how the bandwidth can be reduced by inducing a transverse tilt to the electron beam (as mentioned earlier, the pulse duration and pulse energy are reduced too). The tilt is created simply by changing the strength of a quadrupole magnet in the energy collimator. The pulse energy is measured [41,44] to be around 400 μJ for both the standard case and the large bandwidth mode at maximum bandwidth. The achieved FWHM bandwidths are 0.23% for the standard operation mode and up to 1.66%

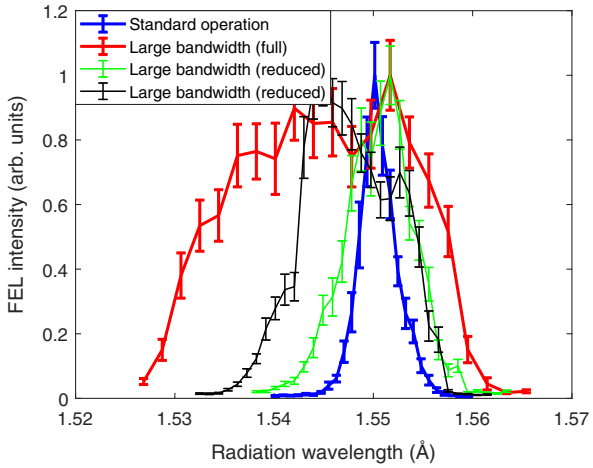

FIG. 5. Measured spectra for standard and large bandwidth operation modes.

for the large bandwidth mode—the full bandwidth for this case is larger than 2%. Hence, the bandwidth increase from standard to large bandwidth operation is more than a factor of 7.

We have established the large bandwidth operation mode several times for radiation wavelengths of 1 to 2 Å, always reproducing equivalent results: spectral bandwidth around 2% with a total pulse energy of few hundred microjoules (corresponding to the pulse energy for standard operation). The maximum achieved FWHM bandwidth was 2.2% for a central radiation wavelength of 1.7 Å and an electron beam energy of 5 GeV. Once the standard operation mode is established, setting up the large bandwidth mode typically takes about one hour.

Our results were obtained with beam energies between 5 and 5.5 GeV, close to the maximum nominal beam energy of SwissFEL. To obtain shorter wavelengths we would operate at lower undulator field (smaller K) but equal electron beam energy [see Eq. (1)]. Such an approach would not affect the relative energy chirp of the electron beam, thereby yielding the same relative radiation bandwidth. For longer wavelengths we would keep the same undulator field K but lower the mean energy of the electron beam [see again Eq. (1)], achieved by simply reducing the voltage of the rf accelerating structures of the main linac. Considering that the absolute energy chirp would not be affected, we expect the relative energy chirp and the bandwidth to increase according to Eq. (1). Starting from the demonstrated 2.2% bandwidth for a wavelength of 1.7 Å (with an electron beam energy of 5 GeV), the relative bandwidth at 7 Å would be doubled to 4.4% (for a beam energy of 2.5 GeV). For the wavelengths between 1.7 and 7 Å, the bandwidth would vary between 2.2 and 4.4% following the dependence shown in Eq. (1). In short, SwissFEL can generate FEL pulses with bandwidth between 2% (for short wavelengths) and 4% or more (for long wavelengths).

The maximum obtained bandwidths qualitatively agree with the ones anticipated in numerical simulations [26]. The obtained values are, however, larger in measurements than in simulations (≈2% compared to ≈1.5%). This is because the experimental chirps of the electron beam are larger than the ones obtained in the numerical calculations (1.54% in the example of Fig. 2 compared to 1.07% in simulations). We attribute this difference to a larger contribution of the linac wakefields (to the energy chirp) in the experiment than what was assumed in the simulations. The conversion from energy chirp to final bandwidth is less efficient in measurements than in simulations: in the results shown in Figs. 2 and 5, the ratio between bandwidth and energy chirp is 1.08, while in simulations it was 1.36. We attribute this difference to a deterioration of the beam quality at the head and tail of the bunch (such as the increase of slice emittance at the tail observed in Fig. 4), and to the fact that the undulator wakefields may not be completely compensated by undulator tapering at the head and tail of the bunch. A detailed study of the undulator wakefields and tapering optimization could lead to even larger bandwidths than presented here.

The large bandwidth radiation generated at SwissFEL has already been harnessed in a user experiment. It was demonstrated that the broadband FEL pulses can be exploited to improve the efficiency of serial protein crystallography: with large bandwidth radiation the probability to obtain a Bragg reflection in a single shot increases, thereby reducing the overall number of required FEL pulses to precisely estimate the structure factors of the protein [45]. More scientific users plan to use the large bandwidth operation mode of SwissFEL to exploit its experimental advantages.

To conclude, we have demonstrated the generation of x-ray FEL radiation with tunable bandwidth as large as 2%. Future work will be dedicated to investigate alternative bandwidth tuning methods entailing less reduction in pulse energy and duration. The broadband pulses produced at SwissFEL pave the way for outstanding progress in x-ray science by significantly improving the efficiency of numerous experimental techniques. At SwissFEL, it has already been shown that crystallography can profit from large bandwidth FEL pulses and users are requesting this operation mode to improve the efficiency of their measurements. Moreover, the production of large bandwidth FEL pulses increases the tunability of several two-color methods, improves the SASE operation with a monochromator, and potentially enhances the efficiency of FEL multiplexing.

We acknowledge all the technical groups involved in the operation of SwissFEL, specially the laser, the diagnostics, the rf, and the operation teams. In particular, we thank Chris Milne for the help in setting up the monochromator and the photodiode used in the spectral measurements, A. Malyzhenkov for fruitful discussions, and Thomas Schietinger for improving the language of the manuscript. This work has been supported by the SNF Grant No. 200021 175498.

*eduard.prat@psi.ch

[1] B. W. J. McNeil and N. R. Thompson, Nat. Photonics **4**, 814 (2010).
[2] C. Pellegrini, A. Marinelli, and S. Reiche, Rev. Mod. Phys. **88**, 015006 (2016).
[3] P. Emma *et al.*, Nat. Photonics **4**, 641 (2010).
[4] T. Ishikawa *et al.*, Nat. Photonics **6**, 540 (2012).
[5] H.-S. Kang *et al.*, Nat. Photonics **11**, 708 (2017).
[6] H. Weise and W. Decking, in *Proceedings of the 38th International Free-Electron Laser Conference, Santa Fe, NM, USA, 2017* (JACoW, Geneva, 2018), p. 9.
[7] C. Milne *et al.*, Appl. Sci. **7**, 720 (2017).
[8] A. M. Kondratenko and E. L. Saldin, Part. Accel. **10**, 207 (1980).
[9] R. Bonifacio, C. Pellegrini, and L. M. Narducci, Opt. Commun. **50**, 373 (1984).
[10] J. Amann *et al.*, Nat. Photonics **6**, 693 (2012).
[11] D. Ratner *et al.*, Phys. Rev. Lett. **114**, 054801 (2015).
[12] I. Inoue *et al.*, Nat. Photonics **13**, 319 (2019).
[13] C. Dejoie, L. B. McCusker, C. Baerlocher, R. Abela, B. D. Patterson, M. Kunz, and N. Tamura, J. Appl. Crystallogr. **46**, 791 (2013).
[14] S. Baradaran, U. Bergmann, H. Durr, K. Gaffney, J. Goldstein, M. Guehr, J. Hastings, P. Heimann, R. Lee, M. Seibert, and J. Stohr, SLAC Report No. R-993, 2012.
[15] J. Arthur *et al.*, SLAC Report No. R-1006, 2013.
[16] B. D. Patterson *et al.*, New J. Phys. **12**, 035012 (2010).
[17] S. K. Son, H. N. Chapman, and R. Santra, Phys. Rev. Lett. **107**, 218102 (2011).
[18] D. Zhu *et al.*, Rev. Sci. Instrum. **85**, 063106 (2014).
[19] Y. Feng *et al.*, J. Synchrotron Radiat. **22**, 626 (2015).
[20] E. Prat, M. Calvi, and S. Reiche, J. Synchrotron Radiat. **23**, 874 (2016).
[21] M. Song, J. Yan, K. Li, C. Feng, and H. Deng, Nucl. Instrum. Methods Phys. Res., Sect. A **884**, 11 (2018).
[22] S. Bettoni, E. Prat, and S. Reiche, Phys. Rev. Accel. Beams **19**, 050702 (2016).
[23] A. Saa Hernandez, E. Prat, and S. Reiche, Phys. Rev. Accel. Beams **22**, 030702 (2019).
[24] P. Dijkstal, S. Reiche, and E. Prat, in *Proceedings SPIE 11038, X-Ray Free-Electron Lasers: Advances in Source Development and Instrumentation V* (SPIE, 2019), p. 110380X.
[25] J. L. Turner *et al.*, in *Proceedings of the 36th International Free Electron Laser Conference, Basel, Switzerland, 2014* (JACoW, Geneva, 2015), p. 337.
[26] A. Saa Hernandez, E. Prat, S. Bettoni, B. Beutner, and S. Reiche, Phys. Rev. Accel. Beams **19**, 090702 (2016).
[27] G. Penco, M. Danailov, A. Demidovich, E. Allaria, G. De Ninno, S. Di Mitri, W. M. Fawley, E. Ferrari, L. Giannessi, and M. Trovó, Phys. Rev. Lett. **112**, 044801 (2014).
[28] P. Craievich, Phys. Rev. ST Accel. Beams **13**, 034401 (2010).
[29] P. Emma *et al.*, Phys. Rev. Lett. **112**, 034801 (2014).

[30] S. Antipov, S. Baturin, C. Jing, M. Fedurin, A. Kanareykin, C. Swinson, P. Schoessow, W. Gai, and A. Zholents, Phys. Rev. Lett. **112**, 114801 (2014).
[31] G. Andonian *et al.*, Phys. Rev. Lett. **95**, 054801 (2005).
[32] M. W. Guetg *et al.*, in *Proceedings of the 7th International Particle Accelerator Conference, Busan, Korea, 2016* (JACoW, Geneva, 2016), p. 813.
[33] M. W. Guetg, A. A. Lutman, Y. Ding, T. J. Maxwell, and Z. Huang, Phys. Rev. Lett. **120**, 264802 (2018).
[34] P. Craievich *et al.*, in *Proceedings of the 35th International Free-Electron Laser Conference, New York, USA, 2013* (JACoW, Geneva, 2013), p. 236.
[35] E. Prat *et al.* (to be published).
[36] B. E. Carlsten and T. O. Raubenheimer, Phys. Rev. E **51**, 1453 (1995).
[37] E. L. Saldin, E. A. Schneidmiller, and M. V. Yurkov, Nucl. Instrum. Methods Phys. Res., Sect. A **398**, 373 (1997).
[38] M. W. Guetg, B. Beutner, E. Prat, and Sven Reiche, Phys. Rev. ST Accel. Beams **18**, 030701 (2015).
[39] E. Prat *et al.*, Phys. Rev. Lett. **123**, 234801 (2019).
[40] J. Rehanek *et al.*, J. Instrum. **12**, P05024 (2017).
[41] P. Juranić *et al.*, J. Synchrotron Radiat. **25**, 1238 (2018).
[42] R. Follath, U. Flechsig, C. Milne, J. Szlachetko, G. Ingold, B. Patterson, L. Patthey, and R. Abela, AIP Conf. Proc. **1741**, 020009 (2016).
[43] G. Ingold *et al.*, J. Synchrotron Radiat. **26**, 874 (2019).
[44] K. Tiedtke *et al.*, J. Appl. Phys. **103**, 094511 (2008).
[45] K. Nass *et al.* (to be published).